Journal of Great Lakes Research 42 (2016) 1139–1150

Contents lists available at ScienceDirect

Journal of Great Lakes Research

journal homepage: www.elsevier.com/locate/jglr

A multi-model approach to evaluating target phosphorus loads for Lake Erie

Donald Scavia [a,*], Joseph V. DePinto [b], Isabella Bertani [a]

[a] Graham Sustainability Institute, University of Michigan, 625 East Liberty Road, Ann Arbor, MI 48193, USA
[b] LimnoTech, 501 Avis Drive, Ann Arbor, MI 48108, USA

ARTICLE INFO

Article history:
Received 6 March 2016
Accepted 10 September 2016
Available online 20 September 2016

Communicated by Robert E. Hecky

Index words::
Loading targets
Great Lakes Water Quality Agreement
Lake Erie
Eutrophication models

ABSTRACT

In response to water quality changes in the Great Lakes since implementing the 1978 Amendment to the Great Lakes Water Quality Agreement, the US and Canada renegotiated the agreement in 2012, requiring the governments to review and revise phosphorus (P) load targets, starting with Lake Erie. In response, the governments supported a multi-model team to evaluate the existing objectives and P load targets for Lake Erie and provide the information needed to update those targets. Herein, we describe the process and resulting advice provided to the binational process. The collective modeling effort concluded that avoiding severe Western Basin (WB) cyanobacteria blooms requires: 1) focusing on reducing total P loading from the Maumee River, with an emphasis on high-flow events during March–July, 2) focusing on dissolved reactive P load alone will not be sufficient because there is significant bioavailable P in the particulate phosphorus portion of the load, and 3) loading from the Detroit River is not a driver of cyanobacteria blooms. Reducing Central Basin (CB) hypoxia requires a CB + WB load reduction greater than what is needed to reach the WB cyanobacteria biomass goal. Achieving *Cladophora* thresholds will be challenging without site-specific load reductions, and more research is needed.

Introduction

In response to significant water quality changes in the Great Lakes since implementing the 1978 Amendment to the Great Lakes Water Quality Agreement (GLWQA) (e.g., Evans et al., 2011; IJC, 2014; Scavia et al., 2014), the US and Canada renegotiated the GLWQA (GLWQA, 2012). Annex 4 of the 2012 GLWQA Protocol set interim phosphorus (P) loading targets identical to those established in the 1978 Amendment, and required the US and Canadian governments to review those targets and recommend adjustments if needed, starting with Lake Erie.

As part of the GLWQA review, a committee of modelers examined data and models used to support the P target loads in the 1978 Amendment relative to the current status of the Lakes and models (DePinto et al., 2006). At that time, a set of Great Lakes eutrophication models were used to help establish target P loads designed to eliminate excess algae growth and to reduce areas of low dissolved oxygen (DO) concentration — key eutrophication symptoms at that time. Those models ranged from simple empirical relationships to kinetically complex, process-oriented models (Bierman, 1980; Vallentyne and Thomas, 1978), and post-audit of several of those models confirmed they had established sound relationships between P loading and system-wide averaged P and chlorophyll-*a* concentrations (e.g., Di Toro et al., 1987; Lesht et al., 1991).

However, DePinto et al. (2006) concluded that those models were not resolved enough spatially to capture the characteristics of nearshore eutrophication, nor the impacts of more recent ecosystem changes, such as impacts from dreissenid mussels and other invasive species. Nor were they designed to address harmful algal blooms (HABs). Their recommendation was to establish a new effort to quantify relative contributions of the factors controlling Great Lakes re-eutrophication (Scavia et al., 2014), and to revise quantitative relationships among those stressors and eutrophication indicators such as HABs, hypoxia, and nuisance benthic algae.

In response, several new Great Lakes modeling efforts were initiated, and given the availability of these new models, the parties to the GLWQA, Environment Canada and the US EPA, supported a new team to evaluate the interim P objectives and load targets for Lake Erie and to provide the information needed to update those targets. Herein, we describe that process and the resulting advice provided to the GLWQA process because the Lake Erie plan is intended to also serve as a template for the other Great Lakes.

Approach

Ecosystem Response Indicators

Before initiating the modeling work, Ecosystem Response Indicators (ERIs) and their associated metrics were established with the GLWQA Annex 4 Nutrient Objectives and Targets Task Team (GLWQA, 2015).

* Corresponding author.
E-mail address: scavia@umich.edu (D. Scavia).

http://dx.doi.org/10.1016/j.jglr.2016.09.007
0380-1330/

Four ERIs of Lake Erie eutrophication appropriate for the Annex 4 Objectives were selected:

- *Western Basin (WB) cyanobacteria biomass* represented by the maximum 30-day average cyanobacteria biomass
- *Central Basin (CB) hypoxia* represented by number of hypoxic days; average extent of hypoxic area during summer; and average hypolimnion DO concentration during August and September
- *Basin-specific overall phytoplankton biomass* represented by summer average chlorophyll-*a* concentration
- *Eastern Basin (EB) Cladophora* represented by dry weight biomass and stored P content.

Multi-model strategy

A multi-model approach was used to explore relationships between the ERIs and P loads because a suite of models with a broad range of complexities and approaches affords an informative comparison of results. Bierman and Scavia (2013) and Weller et al. (2013) identified a number of benefits of applying multiple models of differing complexity:

- Problems and data are viewed from different conceptual and operational perspectives
- The level of risk in environmental management decisions is reduced
- Model diversity adds more value to the decision process than model multiplicity
- Findings are stronger when multiple lines of evidence are available
- Using multiple models increases knowledge and understanding of underlying processes
- Average predictions from a set of models are typically better than from a single model
- Information from multiple models can help quantify uncertainty
- Multiple models can expand opportunities for additional stakeholders to participate
- Reconciling differences among models provides insights on key sources and processes

There is also precedent for using multi-model approaches to support management decisions. As noted above, this approach was used in the late 1970′s to establish the original target P loads for the Great Lakes (Bierman, 1980). In that case, the six models ranged in complexity from an empirical steady state model (Vollenweider, 1976) to more complex, mechanistic models of Lake Erie (Di Toro and Connolly, 1980) and Saginaw Bay (Bierman and Dolan, 1981). Additional examples include addressing polychlorinated biphenyls (PCBs) in Lake Ontario (IJC, 1988), and nutrient loads for the Neuse River Estuary (Stow et al., 2003), the Gulf of Mexico (Scavia et al., 2004), and the Chesapeake Bay (Weller et al., 2013).

After establishing the ERIs, model equations, coefficients, driving variables, assumptions, and time step of predictions were described; calibrations, confirmations, and uncertainties/sensitivities were compared; and the ability of each model to develop ERI metric load–response curves was reviewed. With this information and results from previous publications, the model capabilities were reviewed with respect to the following evaluation criteria:

- *Applicability to ERI metrics*: The models' ability to address the spatial, temporal, and kinetic characteristics of the ERI metrics. While models that address other objectives can be informative, highest priority was given to those that can address the ERIs directly.
- *Extent/quality of calibration and confirmation*: Calibration — The models' ability to reproduce ERI metric state-variables and internal processes. Post-calibration testing — The models' ability to replicate conditions not represented in the calibration data set.
- *Extent of model documentation*: The extent of documentation, including descriptions of model kinetics calculations, inputs, calibration, confirmation, and applications.
- *Level of uncertainty analysis*: The extent to which the models evaluated uncertainty and sensitivity, including for example, those associated with measurement error, model structure, parameterization, aggregation, and uncertainty in characterizing natural variability.

The models

The models that satisfied these criteria are summarized in Table 1 and described briefly below. Model formulation, calibration, confirmation, and sensitivity/uncertainty, as well as the construction of load–response curves are provided in more detail in Scavia et al. (2016) and in this issue (Bertani et al., 2016-in this issue; Bocaniov et al., 2016-in this issue; Chapra et al., 2016-in this issue; Rucinski et al., 2016-in this issue; Stumpf et al., 2016-in this issue; Valipour et al., 2016-in this issue; Verhamme et al., 2016-in this issue; Zhang et al., 2016-in this issue), and in Auer et al. (2010), Canale and Auer (1982), Tomlinson et al. (2010) and Lam et al. (2008, 1987, 1983).

Total Phosphorus Mass Balance Model (Chapra et al., 2016-in this issue)

The original version of this parsimonious total phosphorus (TP) mass balance model was used (along with other models) to establish P loading targets for the 1978 Great Lakes Water Quality Agreement. The model has been subsequently revised and updated, including the expansion of the calibration dataset through 2010 and an increase in the post-1990 apparent TP settling velocity to improve model performance, suggesting that mussel invasion may have enhanced the lakes' ability to retain P (Chapra and Dolan, 2012). The model predicts annual average TP concentrations in the offshore waters of the Great Lakes as a function of external load. For Lake Erie, the model computes basin-wide annual average TP concentrations as a function of loads to each basin. In this application, an empirical relationship between summer chlorophyll and TP concentrations derived for each basin was used to predict basin-specific average chlorophyll levels under different TP load scenarios.

U-M/GLERL Western Lake Erie HAB model (Bertani et al., 2016-in this issue)

A probabilistic empirical model developed by Obenour et al. (2014) relates peak summer cyanobacteria biomass in the WB to spring P loading from the Maumee River. The model is calibrated to multiple sets of in situ and remotely sensed bloom observations through a Bayesian hierarchical approach that allows for rigorous uncertainty quantification. The model includes a temporal trend component that suggests an apparent increased susceptibility to cyanobacteria blooms over time. For this application, the original model (Obenour et al., 2014) was modified to include an empirical estimate of the bioavailable portion of the TP load as bloom predictor.

NOAA Western Lake Erie HAB model (Stumpf et al., 2016-in this issue)

This model is based on an empirical regression between spring P load or flow from the Maumee River and peak summer cyanobacteria biomass in the WB as determined through satellite imagery (Stumpf et al., 2012). For this application, the model has been modified to account for the potential difference in cyanobacteria response to load intensity in warm vs. relatively cold early summers. An estimate of bioavailable P load was also tested as bloom predictor.

Nine-box model (Lam et al., 2008, 1987, 1983)

This coarse grid (9-box) P mass balance model was developed to quantify the main physical and biochemical processes that influence Lake Erie eutrophication and related hypoxia (Lam et al., 1983). The model was previously calibrated and validated with water quality observations from 1967 to 1982 (Lam et al., 1987). For this application,

Table 1
Models included in the multi-model effort and Ecosystem Response Indicators (ERIs) addressed by each.

	Ecosystem Response Indicators			
	Basin-specific overall phytoplankton biomass	WB cyanobacteria peak summer biomass	CB hypoxia	EB *Cladophora*
NOAA Western Lake Erie HAB Model		X		
U-M/GLERL Western Lake Erie HAB Model		X		
Total Phosphorus Mass Balance Model	X			
1-D Central Basin Hypoxia Model	X (CB only)		X	
Ecological Model of Lake Erie (EcoLE)	X (WB only)		X	
Nine-box Model			X	
Western Lake Erie Ecosystem Model (WLEEM)	X (WB only)	X		
ELCOM-CAEDYM	X		X	X
Great Lakes *Cladophora* Model (GLCM)				X

the original calibration was modified to account for changes in settling and re-suspension processes due to dreissenid mussel invasion as described in Scavia et al. (2016).

1-Dimensional Central Basin hypoxia model (Rucinski et al., 2016-in this issue)

A one-dimensional linked vertical hydrodynamic and eutrophication model was previously developed, calibrated, and corroborated with water quality observations in the CB (Rucinski et al., 2014, 2010). The model is driven by a 1-D hydrodynamic model that provides temperature and vertical mixing profiles. The biological portion of the model incorporates P and carbon (C) loading and internal cycling, algal growth and decay, zooplankton grazing, water column oxygen consumption and production processes, and sediment oxygen demand (SOD). The model has been tested with 19 years (1987–2005) of observed loading rates and meteorological conditions to understand the relative contribution of stratification conditions versus P loading extent and seasonal timing on the severity of hypoxia in the CB.

Ecological model of Lake Erie — EcoLE (Zhang et al., 2016-in this issue)

A two-dimensional hydrodynamic and water quality model based on the CE-QUAL-W2 framework was developed and applied to Lake Erie (Zhang et al., 2008). The model was calibrated with observations from 1997 and verified with data collected in 1998 and 1999. The model has been used to estimate the impact of grazing and nutrient excretion by dreissenid mussels on phytoplankton biomass and seasonal succession (Zhang et al., 2011). As part of this application, the model was also used to estimate the spatial distribution and relative contribution of different external and internal P sources to the overall P lake budget.

Western Lake Erie Ecosystem Model — WLEEM (Verhamme et al., 2016-in this issue)

The Western Lake Erie Ecosystem Model (WLEEM) is a three-dimensional, fine-scale, process-based, linked hydrodynamic-sediment transport-eutrophication model developed to simulate water quality responses to changes in meteorological conditions and loads of water, sediments, and nutrients to the WB. The numerous state variables encompass three phytoplankton groups, including cyanobacteria. In this application, the model was used to simulate the response of WB summer cyanobacteria biomass to a broad suite of P load scenarios, including assessing the impact of potential load reduction strategies selectively targeting specific tributaries or specific P forms (dissolved reactive P (DRP) vs. TP).

ELCOM-CAEDYM (Bocaniov et al., 2016-in this issue)

This is a three-dimensional hydrodynamic and ecological model that dynamically couples a hydrodynamic model (Hodges et al., 2000) with a bio-geochemical model (Hipsey, 2008). The model was calibrated and applied to Lake Erie to explore the effect of mussel grazing on phytoplankton biomass, the sensitivity of thermal structure to variations in meteorological parameters, the effects of winter ice on water quality parameters, and the variability in hypoxic area extent as a function of bottom water DO concentration (Bocaniov and Scavia, 2016; Bocaniov et al., 2014; Leon et al., 2011; Liu et al., 2014; Oveisy et al., 2014). As part of this application, different DO concentration thresholds (1–4 mg/L) were used for defining hypoxia when comparing P loading scenarios.

Eastern Basin Cladophora modeling

The Annex 4 multi-model work for this ERI was conducted using the Great Lakes *Cladophora* Model (Auer et al., 2010). This model simulates biological processes driving *Cladophora* biomass and stored P, and it predicts *Cladophora* standing crop as a function of depth, light, temperature, and DRP concentration. The model was originally calibrated and verified with data from Lake Huron and Lake Michigan (Tomlinson et al., 2010). For the Annex 4 analysis, the model was applied to Lake Erie's EB (see Scavia et al., 2016) and results relating *Cladophora* biomass to in-lake DRP concentrations were linked to output from the Total Phosphorus Mass Balance Model and an empirical relationship between TP and DRP concentrations 2016. Because of the insufficient time, resources, and data available in the time frame of the Annex 4 work plan, it was recognized that this generic application was a preliminary estimate and that additional site-specific research, monitoring, and modeling would be needed to obtain a more confident estimate of target P loads for the Eastern Basin. In response, following the Annex 4 work, Valipour et al. (2016-in this issue) linked the *Cladophora* Growth Model (GCM) (Higgins et al., 2006) with a high-resolution 3-D hydrodynamic and water quality model (ELCOM-CAEDYM) to evaluate the fine-scale response of *Cladophora* biomass along the northern shoreline of the EB to changes in external phosphorus loads. While results from this work were not available at the time of the original multi-model effort, they provide relevant new insight on the relative contribution of local tributary loads vs. offshore-nearshore nutrient exchanges to *Cladophora* growth in the EB of Lake Erie.

Phosphorus loadings and scenarios

All of the models include P loading as input, and used 2008 loads and conditions as baselines for comparison. Maccoux et al. (2016-in this issue) provide a detailed long-term analysis of TP (1967–2013) and DRP (2009–2013) loads delivered annually to Lake Erie. The analysis confirms that after a period of gradual decline in the 70s and early 80s, TP loads have shown high year-to-year variation, but no clear long-term trend. Inter-annual variability is largely driven by hydrometeorological conditions, which modulate the timing and magnitude of surface runoff and ultimately the amount of nutrients delivered to the lake (Dolan and Richards, 2008). During 2003–2013, TP from non-point sources contributed on average 71% of the total annual load, while point sources accounted for 19% and atmospheric load and inputs

from Lake Huron made up the remaining 10%. TP loads differ substantially among basins, with the WB receiving on average 60% of the whole lake load, and the CB and EB receiving 28% and 12%, respectively. For 2003–2013, annual loads to the three basins ranged between 487 and 1854 metric tons (MT) in the EB (average: 1059 MT), 1411–3703 MT in the CB (average: 2551 MT), and 3941–7080 MT in the WB (average: 5493 MT).

DRP represented on average 30% of the TP load during 2009–2013, with the WB receiving on average 66% of the whole lake DRP load and the CB and EB receiving approximately 26% and 9%, respectively. Non-point and point sources contributed on average 49% and 39% of the total annual DRP load, respectively, with atmospheric sources and loads from Lake Huron making up the remaining 12%.

The large TP and DRP loads delivered to the WB derive overwhelmingly from two major sources: the Maumee and Detroit rivers. The vast majority of the P delivered by the Maumee River originates from agricultural sources (Han et al., 2012), which dominate the watershed, and are the primary cause of the extremely high TP concentrations in the Maumee (and other WB tributaries) compared to the Detroit River (Fig. 1). As shown in Fig. 1, the Detroit River P concentration is well below that required for producing a cyanobacteria bloom.

While agricultural non-point sources are also primarily responsible for high DRP concentrations in the Maumee, point source contributions result in relatively large DRP loads in the Detroit River as well (Maccoux et al., 2016-in this issue). As a consequence, while the Maumee River contributes only about 5% of the total flow into the WB, it contributes approximately 48% of the TP load and 31% of the DRP load. On the other hand the Detroit River contributes 41% and 59% of the TP and DRP load, respectively, despite accounting for over 90% of the flow (IJC, 2014; Maccoux et al., 2016-in this issue).

A recent long-term (1975–2013) analysis of the Maumee River discharge and nutrient loads showed that while TP concentrations remained stable since the 1990s, DRP concentrations have increased (Stow et al., 2015). However, the authors also show that both TP and DRP loads have increased since the 1990s as a result of a concurrent increase in river discharge. The analysis also suggests the occurrence of changes in load seasonality over the past two decades, with a gradual increase in March discharge and P loads. This is especially important as both TP and DRP loads tend to peak in March while typically showing relatively low values from July to October (Stow et al., 2015).

Long-term and seasonal changes in the Maumee DRP loads have received increased attention as DRP is generally assumed to be readily available to algae (e.g., Baker et al., 2014a, 2014b). Several algal bioavailability assays conducted in the Maumee River have confirmed that while DRP is virtually 100% bioavailable to algae, the other major fraction of the P load – particulate phosphorus (PP) – is only partially available (DePinto et al., 1981; Young et al., 1985). Results from algal assays were generally consistent with chemical fractionation studies in indicating that approximately 20–40% of the Maumee PP load is bioavailable 2016. Wherever possible, the models included in this effort accounted for the different bioavailability of DRP and PP, either by explicitly incorporating processes contributing to in-lake cycling (e.g., Bocaniov et al., 2016-in this issue; Rucinski et al., 2016-in this issue; Verhamme et al., 2016-in this issue; Zhang et al., 2016-in this issue) or by using the best available knowledge to provide an estimate of the bioavailable fraction of the P load (Bertani et al., 2016-in this issue; Stumpf et al., 2016-in this issue). However, the load–response curves estimated by each model are expressed in terms of TP, the component currently measured by most monitoring programs and directly addressed by the GLWQA Nutrient Annex. In developing loading scenarios, 2008 was chosen as

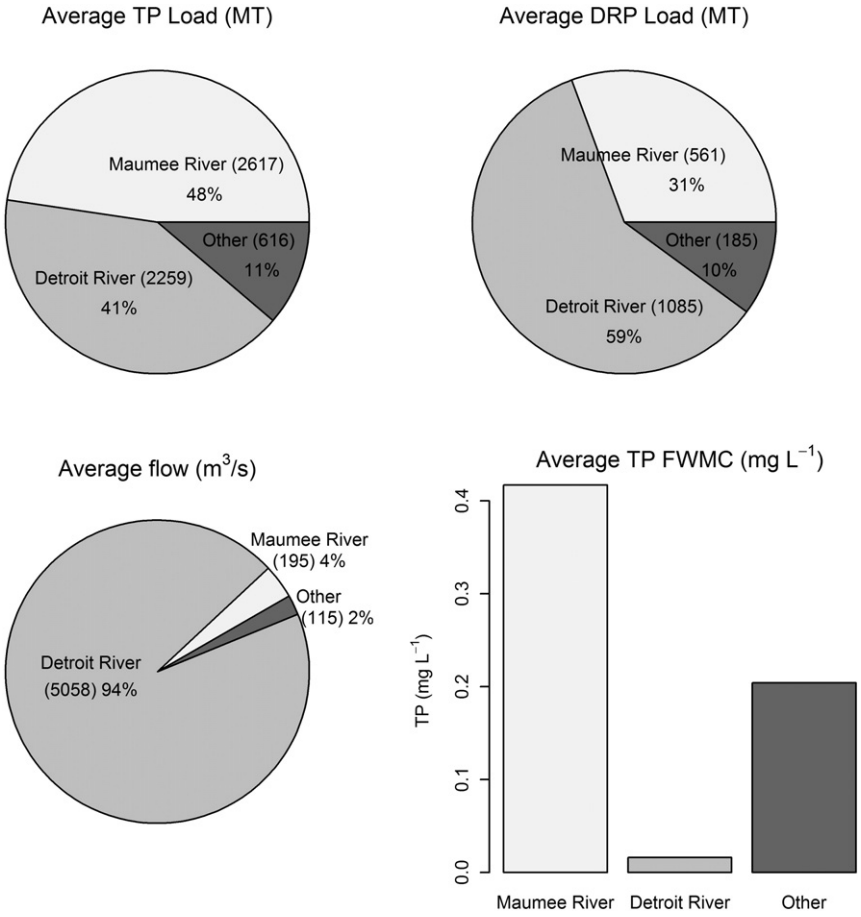

Fig. 1. Annual average TP and DRP loads delivered to the Western Basin by major tributaries (upper panel), and annual average flow (lower left panel) and flow weighted mean TP concentration (FWMC, lower right panel) from the same tributaries.

a baseline year because its load was closest to the original 1978 Annex 3 target of 11,000 MT. At least six load scenarios, defined as 0%, 25%, 50%, 75%, 100%, and 125% of the 2008 TP load, were used to build load–response curves. In some cases, DRP load reductions were also evaluated.

Results and discussion

Load–response curves

Western Basin cyanobacteria summer biomass

The three models used to generate HAB response curves identified P load from the Maumee River as the main driver of bloom size, with relatively similar critical load periods across models (mid-February–June for the Bayesian model; March–July for the other two models) (Fig. 2).

A peak 30-day average cyanobacteria biomass threshold of 9600 MT was selected to provide an illustrative comparison of the effectiveness of load reductions (Table 2). This threshold was chosen because most blooms perceived as "severe" since the early 2000s had satellite-estimated peak 30-day mean bloom sizes >9600 MT.

Differences in model inputs and outputs need to be taken in consideration when comparing response curves. Because the models considered somewhat different loading periods, to facilitate comparisons, spring load is expressed in the response curves as average monthly load (Fig. 2). In addition, the models used different methods to determine peak 30-day average cyanobacteria biomass. The satellite-derived estimates of maximum 30-day average bloom size used by the empirical models are calculated from consecutive 10-day composite images, which are in turn obtained by summing the highest biomass values observed at each pixel over each 10-day period (Stumpf et al., 2012). WLEEM, on the other hand, simulates daily average basin-wide cyanobacteria biomass, from which the maximum 30-day moving average is calculated (Verhamme et al., 2016-in this issue). As a result, a satellite-derived bloom size of 9600 MT corresponds to a lower WLEEM-computed bloom size. To account for this, an adjustment was made to convert the satellite-derived threshold of 9600 MT (Fig. 2a–b) to a "WLEEM equivalent" of 7830 MT (Fig. 2c) (Verhamme et al., 2016-in this issue).

The load–response curves indicate that spring Maumee River TP load reductions below 180 MT/month (Stumpf et al., 2016-in this

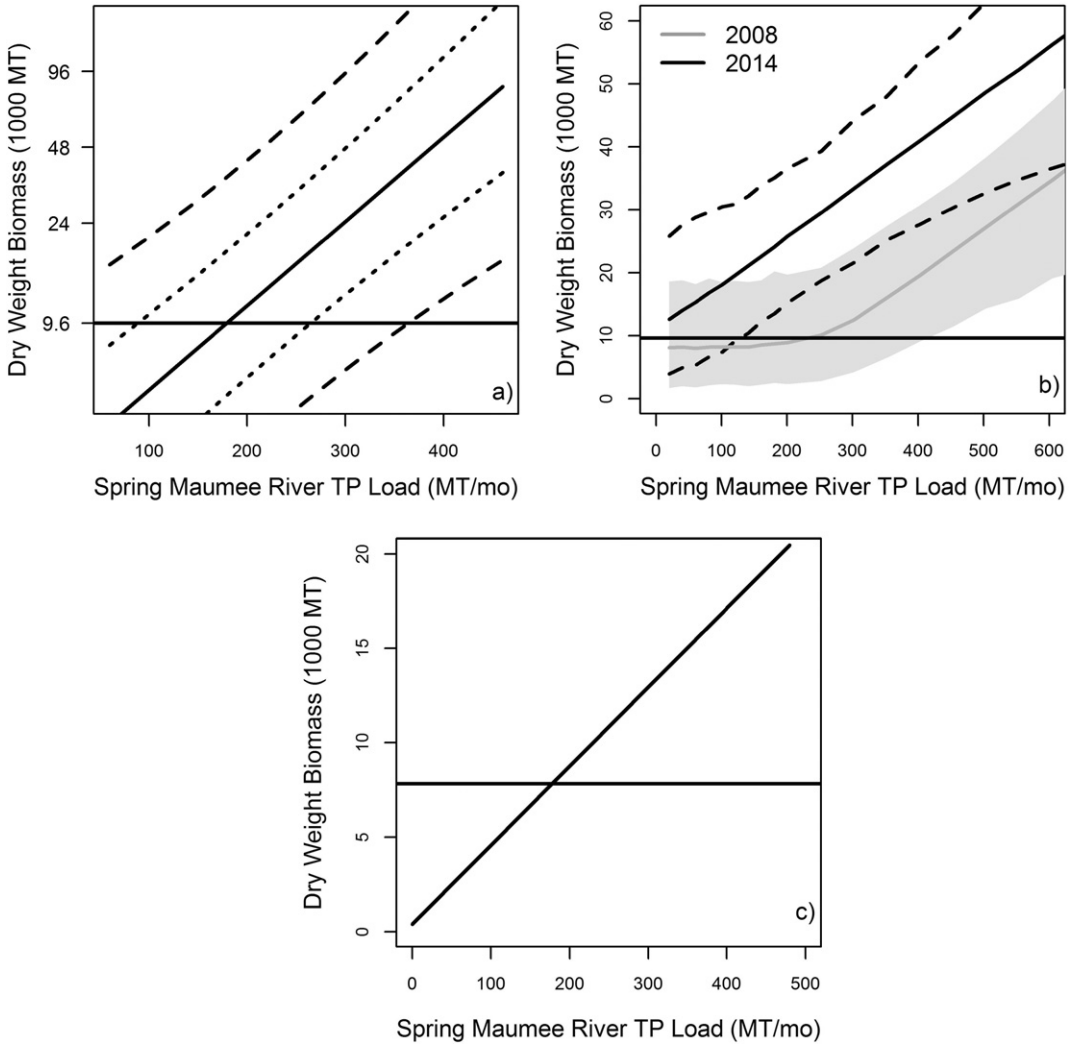

Fig. 2. WB cyanobacteria bloom size predicted by three different models as a function of spring Maumee River TP load: a) NOAA Western Lake Erie HAB model; b) U-M/GLERL Western Lake Erie HAB model; c) Western Lake Erie Ecosystem Model (WLEEM). Solid lines are mean model predictions, while dashed lines and shaded area represent 95% predictive intervals. In a), 70% predictive intervals are also shown as reported in Stumpf et al. (2016-in this issue). In b), model predictions under 2008 (grey) and 2014 (black) lake conditions are shown. Because the models consider different spring load periods (see text), Maumee River load is reported as MT/month to facilitate comparison across models. The horizontal line indicates the threshold for "severe" blooms, which equals 9600 MT for the first two models and was adjusted to an equivalent of 7830 MT for the WLEEM model (see text and Verhamme et al., 2016-in this issue). The corresponding March–July cumulative loads are reported in Table 2.

Table 2
TP loads (MT) associated with example ERI thresholds. Annual Maumee River TP loads corresponding to the suggested March–July loads were calculated assuming the March–July load represents on average 53% of the annual load (data from Heidelberg University's National Center for Water Quality Research, http://tinyurl.com/zgkberb). The corresponding WB annual loads were calculated assuming the Maumee annual load represents on average 48% of the whole WB annual load (Maccoux et al., 2016-in this issue).The whole lake annual loads corresponding to the suggested hypoxia-related WB + CB loads were calculated assuming the WB + CB load represents on average 88% of the whole lake load (Maccoux et al., 2016-in this issue).

Model	Maumee March–July load to achieve threshold	Maumee annual load to achieve threshold	WB annual load to achieve threshold	WB + CB annual load to achieve threshold	Whole lake annual load to achieve threshold
Loads to reduce Western Basin					
UM/GLERL_2008	1150	2170	4520		
NOAA	900	1698	3538		
WLEEM	890	1679	3498		
Mean ± st. dev.	980 ± 147	1849 ± 278	3852 ± 579		
Loads to reduce Central Basin hypolimnetic dissolved oxygen to 4 mg/L					
EcoLE_1–3 m				4400	5000
EcoLE_1m				2600	2955
ELCOM-CAEDYM				3100	3523
1D CB Hypoxia_WBconst				5100	5795
1D CB Hypoxia _WLEEM				4000	4545
Mean ± st. dev.				3840 ± 1001	4364 ± 1138
Loads to reduce Central Basin hypoxic area to 2000 km^2					
EcoLE_1–3 m				5955	6767
EcoLE_1m				3415	3881
ELCOM-CAEDYM				4920	5591
1D CB Hypoxia_WBconst				4830	5489
1D CB Hypoxia _WLEEM				3880	4409
Mean ± st. dev.			*omitting 9- Box	4600 ± 989*	5227 ± 1124*
Loads to reduce Cladophora dry weight biomass to 30 g/m^2					
GLCM/ELCOM-CAEDYM					See text

issue), 178 MT/month (Verhamme et al., 2016-in this issue), and 230 MT/month (under 2008 conditions; Bertani et al., 2016-in this issue) result in a mean bloom size below the selected threshold. These monthly loads correspond to cumulative Maumee March–July loads of 890–1150 MT (mean ± st. dev. = 980 ± 147 MT) and to cumulative Maumee annual loads of 1679–2170 MT (mean ± st. dev. = 1849 ± 278 MT) (Table 2).

The models generally agree that both the DRP and PP fractions of the TP load need to be taken into consideration when setting HAB-related load targets and that management strategies focused only on DRP will not likely be sufficient to achieve target bloom sizes (Bertani et al., 2016-in this issue; Verhamme et al., 2016-in this issue). WLEEM also underscores the focus on the Maumee watershed when setting HAB-related load targets (Verhamme et al., 2016-in this issue). Response curves obtained by reducing the Maumee load vs. reducing loads from all WB tributaries are very similar, indicating that load reduction from the Maumee River is by far the most important. Their evaluation of HAB response to Detroit River TP load reductions confirms the negligible role that the Detroit River plays in bloom formation, although loads from the Detroit River do influence other ecosystem properties such as TP, DRP, and total chlorophyll levels in the WB (Verhamme et al., 2016-in this issue), and CB hypoxia (see the "Central Basin hypoxia" section).

Basin-specific overall phytoplankton biomass

A recent long-term analysis of the trophic state of the Great Lakes showed that average summer chlorophyll-*a* concentrations in the CB and EB of Lake Erie rarely exceeded 2.5 μg/L over the past three decades (Dove and Chapra, 2015), indicating that further decreases in summer phytoplankton biomass in these two basins are not needed (Scavia et al., 2016). Load–response curves for total chlorophyll are therefore only presented for the WB, the most productive of the three basins (Dove and Chapra, 2015). An analysis of the basin-specific TP concentrations predicted by the Total Phosphorus Mass Balance model suggested that a 40% reduction from the 2008 WB and CB loads would result in a 25–30% decrease in average spring TP concentrations in each basin (Chapra et al., 2016-in this issue; GLWQA, 2015), thereby most likely preventing significant impacts on the basins' carrying capacity and fish productivity (GLWQA, 2015; Scavia et al., 2016s).

Based on analysis of model performance, four models were judged suitable for exploring the relationship between WB total phytoplankton biomass and external TP loading (Fig. 3). Direct comparisons across load–response curves are difficult because the models used different averaging periods for reporting summer mean chlorophyll-*a* concentrations (Scavia et al., 2016). To facilitate comparisons, chlorophyll concentrations from each model were converted to a percent of the chlorophyll value estimated for the highest load. All response curves were plotted as a function of WB loads (Fig. 3) because CB and EB loads have negligible influence on phytoplankton growth in the WB. Whenever whole lake loads were used in the original model application, they were converted to corresponding WB loads based on the ratio of the 2008 WB load to the whole lake load.

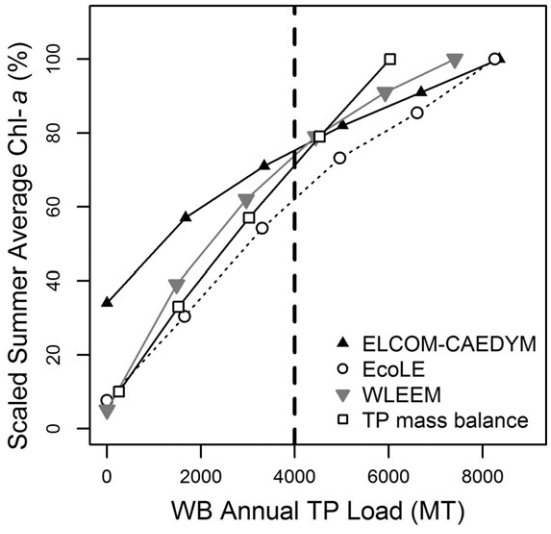

Fig. 3. Average summer chlorophyll-*a* concentration in the WB predicted by different models as a function of annual WB TP loads. Each response curve has been scaled to 100% at its maximum chlorophyll value to facilitate comparisons. The dashed line represents a 40% reduction from the 2008 WB annual load.

These models span a broad range of modeling approaches and complexity. For example, Chapra et al. (2016-in this issue) compute chlorophyll concentrations by combining a parsimonious TP mass-balance model with a relatively simple empirical relationship between August chlorophyll and in-lake TP concentrations. On the other hand, the ELCOM-CAEDYM, EcoLE, and WLEEM models simulate several complex biophysical processes and multiple ecological drivers in addition to P concentrations when predicting chlorophyll-*a*, and their results are averaged over different summer months (June–August for ELCOM-CAEDYM and EcoLE, and July–September for WLEEM). The broad diversity in model formulation, assumptions, and level of complexity provides insight on the range of expected outcomes (Fig. 3). While no specific objective was established for WB total phytoplankton biomass, it is instructive to note that reducing loads to prevent significant HABs (Table 2) would likely reduce total phytoplankton biomass by ca. 25% in the WB.

Central Basin hypoxia

The models used for this ERI were all calibrated and to varying extent confirmed over recent but different time periods, and are therefore good representations of the current state of the system. While most models are vertically resolved into several layers that allow for a fine-scale representation of seasonal variations in DO profiles, the 9-Box model's 2-layer resolution makes comparisons difficult. For this reason, the 9-Box model was not included in the composite recommendations. The hypoxia response curves from each model were plotted as a function of the annual WB + CB TP loads (Fig. 4). When whole lake loads were used in the original model application, they were converted to WB + CB loads based on the ratio of the 2008 WB + CB load to the whole lake load.

The response curves for August–September average hypolimnetic DO concentration (Fig. 4a) show similar decreasing trends with increasing loads. Some of the differences among models, especially at lower loads, could be partly attributed to the fact that the 1-D model simulates horizontally-averaged DO, while the other models simulate horizontally-resolved DO concentrations in the bottom layer (0.5–1.0 m for ELCOM-CAEDYM; 1.0 and 1–3 m for EcoLE). Differences could also be attributed to different formulations of SOD, which becomes more important at lower external loads. The 1-D model (Rucinski et al., 2016-in this issue) also compared two different

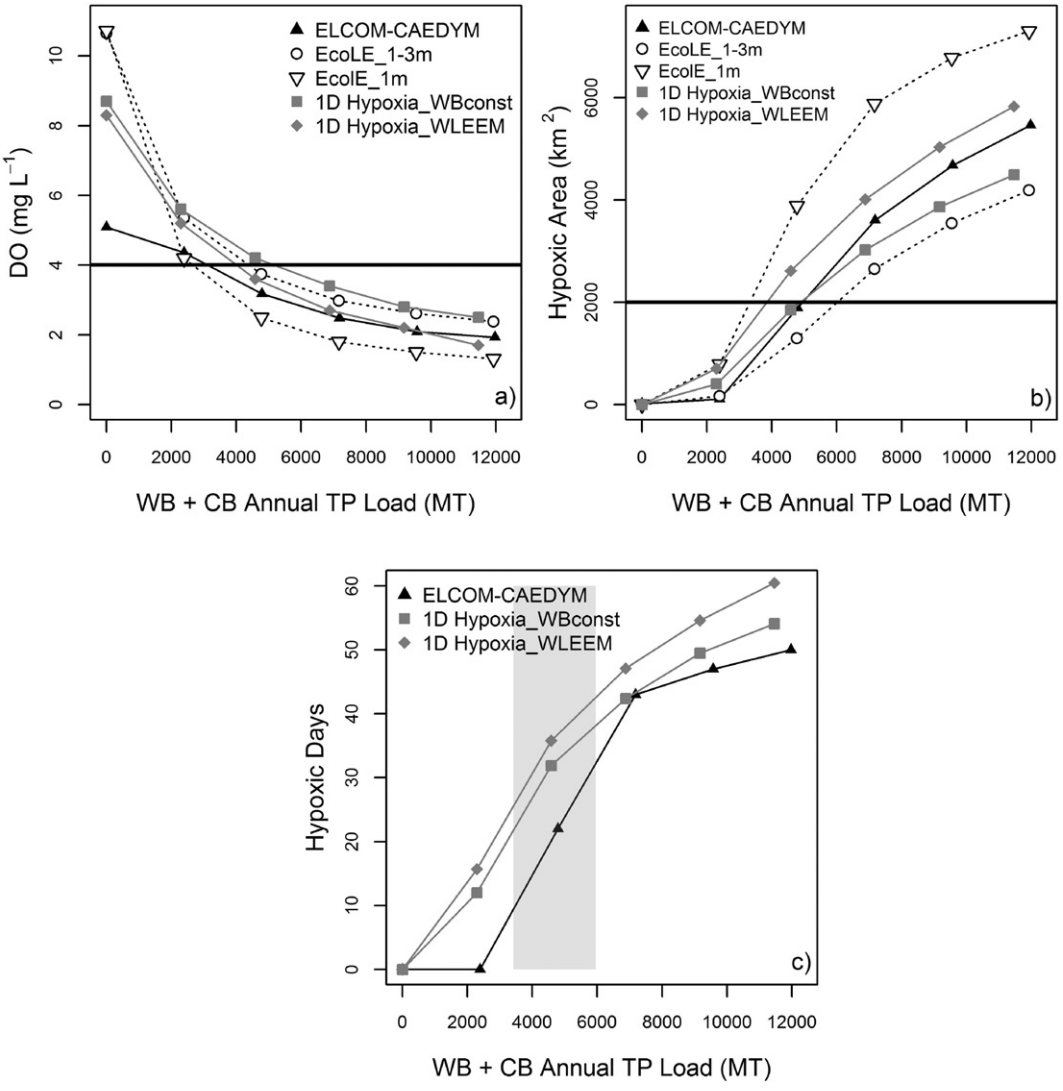

Fig. 4. CB hypoxia metrics predicted by different models as a function of WB + CB annual TP load: a) August–September average hypolimnetic DO concentration in the CB. The horizontal line represents the average concentration (4 mg/L) corresponding to initiation of statistically significant hypoxic areas (Zhou et al., 2013); b) August–September average extent of the CB hypoxic area. The horizontal line indicates a threshold of 2000 km^2; c) Number of hypoxic days in the CB. The shaded area indicates the range of loads required to achieve the hypoxic area threshold of 2000 km^2. Results for the EcoLE model are shown considering a bottom layer of 1 m (EcoLE_1m) and 1–3 m (EcoLE_1–3 m). Results for the 1-D hypoxia model are shown considering a constant net apparent TP deposition rate in the WB (1D Hypoxia_WBconst) and considering TP loads from the WB to the CB as simulated by the WLEEM model (1D Hypoxia_WLEEM).

approaches to estimate loads entering the CB from the WB. One method assumed a constant net apparent TP deposition rate previously estimated for the WB, whereas the alternative approach used nutrient loads from the WB to the CB as simulated by WLEEM. A comparison of the respective load–response curves shows that the two methods yield similar results (Fig. 4).

There is strong convergence among models at more typical loading rates (Fig. 4a). An example hypolimnetic DO concentration threshold of 4.0 mg/L was selected to compare model predictions because, while hypoxia is typically defined as DO below 2.0 mg/L, Zhou et al. (2013) showed that statistically significant hypoxic areas start to occur when average hypolimnetic water DO concentrations during the summer stratified period are below approximately 4 mg/L. Using that as an example target threshold, model predictions suggest reducing the WB + CB load to below 2600–5100 MT (mean ± st. dev. = 3840 ± 1001; Table 2).

The models were also used to relate loads to hypoxic area (area with DO concentration <2 mg/L). ELCOM-CAEDYM estimates this metric directly through its fine-scale 3-D approach; the other two models use the empirical relationship between hypoxic area and bottom-layer DO concentration developed by Zhou et al. (2013). As expected, all models show that hypoxic extent decreases with decreasing TP loads (Fig. 4b), and suggest that decreasing the annual WB + CB TP load to 3415–5955 MT (mean ± st. dev. = 4600 ± 989 MT) is needed to reduce the average hypoxic extent to 2000 km^2 (Fig. 4b and Table 2), a value typical of the mid-1990s that coincides with a period of recovery of several recreational and commercial fisheries in Lake Erie's WB and CB (Ludsin et al., 2001; Scavia et al., 2014).

The models also estimated the influence of load reductions on the number of hypoxic days (number of days when average bottom water DO is <2 mg/L) (Fig. 4c). The models indicate that a WB + CB TP load below 3415–5955 MT/year would result in a decrease in the number of hypoxic days to between 9 and 42 (Fig. 4c).

The 1-D model simulated hypoxia response to load reductions under the broad range of meteorological conditions observed between 1987 and 2005 (Rucinski et al., 2016-in this issue). Results indicate that the response to load reductions may show substantial inter-annual variability due to meteorological forces driving mixing regimes. These findings are especially relevant in view of projected changes in future climate conditions, which could result in substantial deviations in the lake's behavior from average model predictions. This uncertainty calls for an adaptive management approach, where the system's response to load reductions is assessed over time and new knowledge is used to regularly update models and management strategies. Rucinski et al. (2016-in this issue, 2014) also showed that variations in the lake's thermal structure produced far more inter-annual variability in hypoxic area than variations in the timing, or seasonality, of the load.

Eastern Basin Cladophora

For this ERI, the Great Lakes *Cladophora* Model (Canale and Auer, 1982; Tomlinson et al., 2010) met the criteria required for inclusion in this effort, and while initial results were not used for setting loading targets (see below), it did provide a preliminary estimate. Subsequently, additional site-specific modeling efforts have begun for this portion of the lake, and one of them, a three dimensional hydrodynamic-water quality model by Valipour et al. (2016-in this issue) is presented in this special series.

For Annex 4 work (see Scavia et al., 2016), the Great Lakes *Cladophora* model relating algal biomass to EB DRP concentrations, an empirical model relating DRP to TP concentrations (Dove and Chapra, 2015), and the Total Phosphorus Mass Balance Model (Chapra et al., 2016-in this issue) relating TP concentrations to external TP loads were combined to generate a *Cladophora* biomass-TP load–response curve. Since there is currently no regulatory guidance on acceptable levels of *Cladophora* biomass, a biomass of 30 g dry weight (DW)/m^2 was suggested as a threshold likely to prevent nuisance conditions (Scavia et al., 2016), and that corresponds to DRP and TP concentrations of 0.9 μg P/L and 6.3 μg P/L, respectively, or a whole-lake TP load below 7000 MT/Year. It is important to note that this combined modeling approach was used because of time, resource, and data limitations, and it is not site-specific; but rather relates *Cladophora* biomass along the entire north shoreline of the EB to average offshore nutrient concentrations. However, *Cladophora* proliferates in the nearshore, where it is often subjected to direct impacts of point-source and tributary inputs. Nutrient concentrations in the nearshore waters may therefore be higher and more variable than those in the offshore, and as offshore DRP concentrations are reduced, control of *Cladophora* growth is expected to shift toward nearshore inputs, requiring spatially explicit models.

Some of these limitations were recently addressed by Valipour et al. (2016-in this issue). Their 3-D model simulated the predominant physical processes within the *Cladophora* habitat zone (0–8 m depth) in the EB of Lake Erie, with a focus on the northern coast in the vicinity of the Grand River where *Cladophora* is abundant. Model output was input to the Higgins *Cladophora* Growth Model (CGM) (Higgins et al., 2006) to relate nearshore *Cladophora* biomass to external phosphorus loads. Results showed that while P load reductions can be expected to reduce *Cladophora* biomass in the EB, achieving proposed biomass thresholds may be more challenging than previously thought (Fig. 5). Coastal upwelling events often input significant nutrients along much of the north shore, particularly during May and June when conditions are optimal for *Cladophora* growth. Simulations confirmed that P supplies from both the offshore and local sources (e.g. the Grand River) are capable of generating biomass above the proposed threshold in the vicinity of the Grand River. The relative importance of offshore-nearshore nutrient exchanges vs. local tributary inputs in driving nearshore P concentrations and *Cladophora* growth varies within and across years, most likely resulting in substantial variability in *Cladophora* response as whole lake loads are reduced. Generally, these results indicate that measures aimed at decreasing *Cladophora* biomass in the EB of Lake Erie should take into account nutrient sources from both the offshore region and local tributary inputs (Valipour et al., 2016-in this issue). These results also point to a need for an adaptive management plan for Eastern Basin *Cladophora* that includes research, monitoring, and modeling.

Benefits of the multi-model approach and future research needs

Although the models vary substantially in formulations, assumptions, and parameterizations, the load–response curves generally showed considerable agreement, providing confidence in the robustness of the recommendations. However, quantifying each model's uncertainty explicitly would have further enhanced confidence (Kim et al., 2014). While such quantification is easily accommodated in some models, it is much more difficult, if even possible, for others. The HAB models provide an example. They range from a parsimonious empirical Bayesian hierarchical model capable of accounting quantitatively for model error, bloom measurement error, and uncertainty in parameter estimates to a complex process-based deterministic model that provides model uncertainty in terms of quantitative comparisons of simulations and field observations for all years simulated, but is too complex and runtime consuming for a full Monte Carlo uncertainty analysis. While this illustrates a trade-off between providing causal understanding of ecosystem behavior and rigorously quantifying uncertainty, it also highlights one of the benefits of the multi-model approach. In that approach, the range of predicted outcomes illustrates the degree of confidence in our understanding of, and the predictability of, the system's response to loads.

The thorough representation of uncertainty possible with the statistical models also helps identify key scientific gaps limiting our predictive understanding of the system's behavior and can guide future experimental and monitoring efforts. For example, including multiple independent sets of bloom observations in the Bayesian model suggests that uncertainty associated with bloom characterization represents a

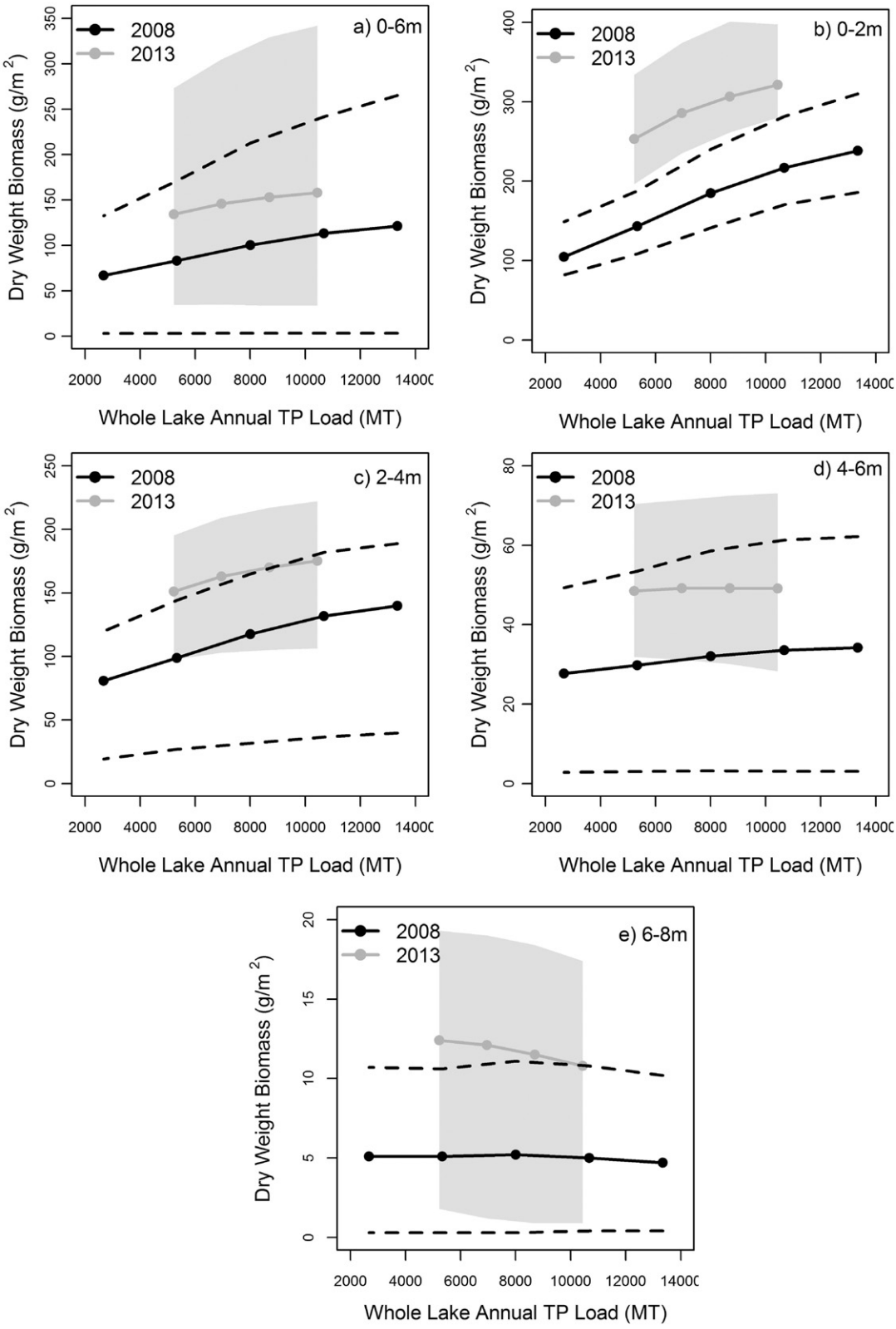

Fig. 5. *Cladophora* biomass predicted by the *Cladophora* Growth Model coupled with the 3-D ELCOM-CAEDYM model in the northern shoreline of the EB as a function of whole lake annual TP load. Load–response curves were developed for two years (2008 and 2013) and at various depth ranges (a–e). For each year and depth range, spatially averaged maximum *Cladophora* biomass and associated 5th and 95th percentiles are shown.

considerable portion of overall HAB predictive uncertainty (Bertani et al., 2016-in this issue). More generally, the relatively large uncertainty in HAB predictions highlights once again the need for adaptive management approaches that track the effectiveness of actions and routinely revise models and management decisions based on new information — a point also emphasized in the analysis of variability associated with meteorology in the 1D hypoxia model (Rucinski et al., 2016-in this issue).

In the case of hypoxia, a key source of uncertainty is quantifying the impact of changes in external loads on SOD. Previous studies have shown that SOD represents a substantial portion of total hypolimnetic oxygen demand in the CB (Rucinski et al., 2014), and both SOD and water column oxygen demand are affected by external loads. The hypoxia models used similar approaches to approximate the potential effects of changes in nutrient loads on future SOD. Rucinski et al. (2016-in this issue) coupled a relationship between SOD and organic carbon sedimentation rates (Borsuk et al., 2001) with a relationship between P loading and carbon settling from his model to predict future SOD as a function of P loads (Rucinski et al., 2014). Bocaniov et al. (2016-in this issue) and Zhang et al. (2016-in this issue) used the relationship developed by Rucinski et al. (2014), but allowed for adjustments to temperature and bottom water DO concentrations. These approaches represent our best available estimates of how SOD rates may change as a function of nutrient loads. However, future research should focus on developing long-term measurement and modeling approaches that can improve our understanding of how SOD and benthic nutrient fluxes will change as a result of external load reductions and how accumulation of nutrients and organic matter in the sediments may delay the system's response to load reductions.

Valuable insight on critical research gaps can also be gained by exploring discrepancies among the models. For example, comparison of the HAB models suggests that quantifying the contribution of the PP component of the TP load in fueling HABs remains a critical challenge. Numerous studies have quantified the algal availability of PP in the Maumee River (see review in Bertani et al., 2016-in this issue; DePinto et al., 1981; Young et al., 1985), and this knowledge has been incorporated in all three HAB models through various approaches. However, we still have limited observational knowledge of the ultimate fate of PP as it is delivered to the lake and undergoes processes that influence its bioavailability, including settling, re-suspension, microbial mineralization, and re-cycling by dreissenid mussels and other organisms. Stumpf et al. (2016-in this issue) explicitly account for the proportion of the Maumee PP load that is assumed to settle out of the water column before reaching the WB open waters based on a recent field study (Baker et al., 2014b). However, field studies exploring nutrient transport dynamics along the river-lake continuum in western Lake Erie are sparse, and more research is needed to quantify physical processes controlling the ultimate fate of riverine nutrients. The 3-D mechanistic models (e.g., Bocaniov et al., 2016-in this issue; Verhamme et al., 2016-in this issue; Zhang et al., 2016-in this issue) attempt to explicitly characterize nutrient transport, in-lake dynamics of bioavailable P and kinetic conversions among P forms (e.g., mineralization of organic P to orthophosphate, gradient-driven desorption of orthophosphate from inorganic PP). However, additional measurements of *in situ* biophysical processes in both the water column and sediments that can further constrain the models will help reduce uncertainties.

Integrating results from different modeling approaches also allows for exploring processes occurring at different spatio-temporal scales. For example, while the process-based HAB model provides key insight into fine scale bloom spatio-temporal dynamics and underlying mechanisms, the empirical models allow for assessment of system responses at longer time scales. For example, the Bayesian model includes a temporal component that suggests increased susceptibility of western Lake Erie to bloom formation over time, suggesting the same TP load is predicted to trigger a larger bloom under present-day conditions compared to earlier years (Fig. 2b). Specifically, the model predicts that under 2008 lake conditions, March–June Maumee TP loads below 230 MT/mo will prevent severe blooms, while under 2014 conditions a TP load of 230 MT/month would still result in an average bloom size of 28,000 MT (95% predictive interval: 17,000–38,000 MT) (Fig. 2b). This temporal trend term, estimated by the Bayesian model, remains significantly positive even after accounting for concurrent increases in DRP loads, suggesting that the observed increase in DRP load alone may not be sufficient to explain the apparent enhanced susceptibility. However, results from the other empirical model do not support these findings. They suggest that removing the influence of the July load for relatively cold years prevents under prediction of some of the most recent blooms (Stumpf et al., 2016-in this issue). Further research is needed to assess whether the lake is becoming more susceptible to bloom formation and, if so, to identify underlying mechanisms, including the role of changes in frequency, magnitude, and timing of extreme weather events (Michalak et al., 2013), the potential impact of selective grazing and nutrient excretion by dreissenid mussels (Arnott and Vanni, 1996; Conroy et al., 2005; Jiang et al., 2015; Vanderploeg et al., 2001; Zhang et al., 2011), the influence of internal loading of both nutrients and cyanobacteria cell inocula (Chaffin et al., 2014b; Rinta-Kanto et al., 2009), the role of nitrogen co-limitation (Chaffin et al., 2014a, 2013; Harke et al., 2015), and the influence of changes in the proportion of available vs. non-available fractions of the TP load (Baker et al., 2014a; Kane et al., 2014).

Conclusions

The load–response curves presented herein represent our current best estimates of how Lake Erie's ERI metrics will respond to changes in P loads, with the loadings necessary to achieve the example thresholds summarized in Table 2. Results of this multi-model approach suggest:

- Achieving Western Basin cyanobacteria biomass reduction requires a focus on reducing TP loading from the Maumee River, with an emphasis on high-flow events during March–July. Results suggest that focusing on Maumee DRP load alone will not be sufficient and that P load from the Detroit River is not a driver of cyanobacteria blooms.
- Reducing Central Basin hypoxia requires a Central + Western Basin annual load reduction greater than what is needed to reach the Western Basin cyanobacteria biomass goal. Load reductions focused on dissolved oxygen concentration and hypoxic areal extent also result in shorter hypoxia duration.
- While the original Annex 4 analysis indicated that the load reductions suggested for meeting the cyanobacteria and Central Basin hypoxia thresholds would be sufficient to meet the Eastern Basin *Cladophora* biomass goal, more recent work (Valipour et al., 2016-in this issue) does not support this conclusion.

These results offered several strategies for setting loading targets under the GLWQA. The thresholds in Table 2 were intended to illustrate the range of load reductions likely needed. They were used by the Objectives and Targets Task Team in their recommendations to the GLWQA Nutrient Annex Subcommittee on loading targets (GLWQA, 2015). Their recommendations, in the context of our findings, were:

- *Western Basin Cyanobacteria* — To keep blooms below 9600 MT algal dry weight (the size of the blooms observed in 2004 or 2012) 90% of the time, the Task Team recommended a Maumee River March–July TP load of 860 MT and a DRP load of 186 MT, consistent with our findings. These loads represent roughly 40% reductions from the 2008 spring loads and correspond to Flow Weighted Mean Concentrations (FWMC) of 0.23 mg/L TP and 0.05 mg/L DRP. FWMC was included in the Task Team recommendation to address significant inter-annual variability in Maumee River discharge. It is expected that maintaining those concentrations will result in loads below the targets 90% of the time, if climate change does not alter precipitation patterns. It was also noted that, while reducing DRP will have a greater impact than reducing PP, reducing DRP alone will not be sufficient. The Task Team also recommended 40% reductions for all other WB tributaries and the Thames River.
- *Central Basin Hypoxia* — Our analysis suggested that setting a minimum summer average hypolimnetic DO concentration of 4 mg/L or reducing hypoxia area to less than 2000 km^2 requires average

WB + CB loads of 3840 MT and 4600 MT, respectively (Table 2). The Task Team believed the load reduction to keep summer hypolimnetic DO concentrations at or above 4 mg/L was so restrictive that it might reduce overall productivity and impact fisheries, so they recommended an annual WB + CB TP loading target of 6000 MT, closer to our area-reduction example and expected to maintain summer hypolimnion DO concentrations above 2 mg/L. This load represents a 40% reduction from 2008 WB + CB load levels.

- *Eastern Basin Cladophora* — While the original Annex 4 analysis suggests that the cyanobacteria- and hypoxia-driven load targets are sufficient to achieve a desired reduction in *Cladophora* in the EB, the Task Team was not sufficiently confident in the cascade of models used to set a loading target for *Cladophora* (Task Team, 2015). They pointed to the need to develop a site-specific model for the north shore of the EB that accounts for nutrient exchanges with the open water, load and transport of specific tributaries, and the role of dreissenids to gain more confidence. A spatially-explicit modeling effort was recently developed to address some of these issues (Valipour et al., 2016-in this issue). This work indicates that reducing nearshore *Cladophora* biomass may be more challenging than previously thought, and more research is needed to develop sound recommendations to address *Cladophora* growth in Lake Erie.

Acknowledgments

This work was funded in part by the USEPA under contract EP-R5-11-07, Task Order 21 and by the University of Michigan Graham Sustainability Institute.

References

Arnott, D.L., Vanni, M.J., 1996. Nitrogen and phosphorus recycling by the zebra mussel (*Dreissena polymorpha*) in the western basin of Lake Erie. Can. J. Fish. Aquat. Sci. 53, 646–659.

Auer, M., Tomlinson, L., Higgins, S., Malkin, S., Howell, E., Bootsma, H., 2010. Great Lakes Cladophora in the 21st century: same alga — different ecosystem. J. Great Lakes Res. 36, 248–255.

Baker, D.B., Confesor, R.B., Ewing, D.E., Johnson, L.T., Kramer, J.W., Merryfield, B.J., 2014a. Phosphorus loading to Lake Erie from the Maumee, Sandusky and Cuyahoga rivers: the importance of bioavailability. J. Great Lakes Res. 40, 502–517.

Baker, D.B., Ewing, D.E., Johnson, L.T., Kramer, J.W., Merryfield, B.J., Confesor, R.B., Richards, R.P., Roerdink, A.A., 2014b. Lagrangian analysis of the transport and processing of agricultural runoff in the lower Maumee River and Maumee Bay. J. Great Lakes Res. 40, 479–495.

Bertani, I., Obenour, D.R., Steger, C.E., Stow, C.A., Gronewold, A.D., Scavia, D., n.d., 2016. Probabilistically assessing the role of nutrient loading in harmful algal bloom formation in western Lake Erie. J. Great Lakes Res. 42 (6), 1184–1192 (in this issue).

Bierman, V., 1980. A Comparison of Models Developed for Phosphorus Management in the Great Lakes. Conference on Phosphorus Management Strategies for the Great Lakes, pp. 1–38.

Bierman, V.J., Dolan, D.M., 1981. Modeling of phytoplankton-nutrient dynamics in Saginaw Bay, Lake Huron. J. Great Lakes Res. 7, 409–439. http://dx.doi.org/10.1016/S0380-1330(81)72069-0.

Bierman, V., Scavia, D., 2013. Hypoxia in the Gulf of Mexico: Benefits and Challenges of Using Multiple Models to Inform Management Decisions.

Bocaniov, S., Scavia, D., 2016. Temporal and spatial dynamics of large lake hypoxia: integrating statistical and three-dimensional dynamic models to enhance lake management criteria. Water Resour. Res. http://dx.doi.org/10.1002/2015WR018170.

Bocaniov, S., Smith, R., Spillman, C., Hipsey, M., Leon, L., 2014. The nearshore shunt and the decline of the phytoplankton spring bloom in the Laurentian Great Lakes: insights from a three-dimensional lake model. Hydrobiologia 731, 151–172.

Bocaniov, S.A., Leon, L.F., Rao, Y.R., Schwab, D.J., Scavia, D., 2016. Simulating the effect of nutrient reduction on hypoxia in a large lake (Lake Erie, USA-Canada) with a three-dimensional lake model. J. Great Lakes Res. 42 (6), 1228–1240 (in this issue).

Borsuk, M., Higdon, D., Stow, C., Reckhow, K., 2001. A Bayesian hierarchical model to predict benthic oxygen demand from organic matter loading in estuaries and coastal zones. Ecol. Model. 143, 165–181.

Canale, R., Auer, M., 1982. Ecological studies and mathematical modeling of *Cladophora* in Lake Huron: 5. Model development and calibration. J. Great Lakes Res. 8, 112–125.

Chaffin, J.D., Bridgeman, T.B., Bade, D.L., 2013. Nitrogen constrains the growth of late summer cyanobacterial blooms in Lake Erie. Adv. Microbiol. 16–26.

Chaffin, J.D., Bridgeman, T.B., Bade, D.L., Mobilian, C.N., 2014a. Summer phytoplankton nutrient limitation in Maumee Bay of Lake Erie during high-flow and low-flow years. J. Great Lakes Res. 40, 524–531. http://dx.doi.org/10.1016/j.jglr.2014.04.009.

Chaffin, J.D., Sigler, V., Bridgeman, T.B., 2014b. Connecting the blooms: tracking and establishing the origin of the record-breaking Lake Erie *Microcystis* bloom of 2011 using DGGE. Aquat. Microb. Ecol. 73, 29–39. http://dx.doi.org/10.3354/ame01708.

Chapra, S.C., Dolan, D.M., 2012. Great Lakes total phosphorus revisited: 2. Mass balance modeling. J. Great Lakes Res. 38, 741–754. http://dx.doi.org/10.1016/j.jglr.2012.10.002.

Chapra, S., Dolan, D., Dove, A., 2016. Mass-balance modeling framework for simulating and managing long-term water quality for the lower Great Lakes. J. Great Lakes Res. 42 (6), 1166–1173 (in this issue).

Conroy, J.D., Edwards, W.J., Pontius, R.A., Kane, D.D., Zhang, H., Shea, J.F., Richey, J.N., Culver, D.A., 2005. Soluble nitrogen and phosphorus excretion of exotic freshwater mussels (*Dreissena* spp.): potential impacts for nutrient remineralisation in western Lake Erie. Freshw. Biol. 50, 1146–1162.

DePinto, J.V., Young, T.C., Martin, S.C., 1981. Algal-available phosphorus in suspended sediments from Lower Great Lakes tributaries. J. Great Lakes Res. 7, 311–325.

DePinto, J.V., Lam, D., Auer, M.T., Burns, N., Chapra, S.C., Charlton, M.N., Dolan, D.M., Kreis, R., Howell, T., Scavia, D., 2006. Examination of the Status of the Goals of Annex 3 of the Great Lakes Water Quality Agreement.

Di Toro, D.M., Connolly, J.P., 1980. Mathematical Models of Water Quality in Large Lakes. Part 2: Lake Erie. EPA-600/3-80-065 Report, Duluth, MN.

Di Toro, D.M., Thomas, N.A., Herdendorf, C.E., Winfield, R.P., Connolly, J.P., 1987. A post audit of a Lake Erie eutrophication model. J. Great Lakes Res. 13, 801–825.

Dolan, D., Richards, R., 2008. Analysis of Late 90s Phosphorus Loading Pulse to Lake Erie. In: Munawar, M., Heath, R. (Eds.), Checking the Pulse of Lake Erie. Aquatic Ecosystem Health and Management Society, Burlington, Ontario, pp. 79–96.

Dove, A., Chapra, S.C., 2015. Long-term trends of nutrients and trophic response variables for the Great Lakes. Limnol. Oceanogr. 60, 696–721. http://dx.doi.org/10.1002/lno.10055.

Evans, M.A., Fahnenstiel, G., Scavia, D., 2011. Incidental oligotrophication of North American Great Lakes. Environ. Sci. Technol. 45, 3297–3303. http://dx.doi.org/10.1021/es103892w.

GLWQA, 2012. The 2012 Great Lakes Water Quality Agreement — Annex 4. http://tinyurl.com/gt92hrh (Viewed 25 February 2016).

GLWQA, 2015. Recommended Phosphorus Loading Targets for Lake Erie — Annex 4 Objectives and Targets Task Team Final Report to the Nutrients Annex Subcommittee.

Han, H., Allan, J., Bosch, N., 2012. Historical pattern of phosphorus loading to Lake Erie watersheds. J. Great Lakes Res. 38, 289–298.

Harke, M.J., Davis, T.W., Watson, S.B., Gobler, C.J., 2015. Nutrient-controlled niche differentiation of western Lake Erie cyanobacterial populations revealed via metatranscriptomic surveys. Environ. Sci. Technol. http://dx.doi.org/10.1021/acs.est.5b03931 (acs.est.5b03931).

Higgins, S.N., Hecky, R.E., Guildford, S.J., 2006. Environmental controls of *Cladophora* growth dynamics in eastern Lake Erie: application of the Cladophora Growth Model (CGM). J. Great Lakes Res. 32, 629–644. http://dx.doi.org/10.3394/0380-1330(2006)32[629:ECOCGD]2.0.CO;2.

Hipsey, M., 2008. The CWR Computational Aquatic Ecosystem Dynamics Model CAEDYM — User Manual. Centre for Water Research, University of Western Australia.

Hodges, B., Imberger, J., Saggio, A., Winters, K., 2000. Modeling basin-scale internal waves in a stratified lake. Limnol. Oceanogr. 1603-1620.

IJC, 1988. Report on Modeling the Loading Concentration Relationship for Critical Pollutants in the Great Lakes. IJC Great Lakes Water Quality Board, Toxic Substances Committee, Task Force on Toxic Chemical Loadings.

IJC, 2014. A Balanced Diet for Lake Erie: Reducing Phosphorus Loadings and Harmful Algal Blooms. Report of the Lake Erie Ecosystem Priority.

Jiang, L., Xia, M., Ludsin, S.A., Rutherford, E.S., Mason, D.M., Marin Jarrin, J., Pangle, K.L., 2015. Biophysical modeling assessment of the drivers for plankton dynamics in dreissenid-colonized western Lake Erie. Ecol. Model. 308, 18–33. http://dx.doi.org/10.1016/j.ecolmodel.2015.04.004.

Kane, D.D., Conroy, J.D., Peter Richards, R., Baker, D.B., Culver, D.A., 2014. Re-eutrophication of Lake Erie: correlations between tributary nutrient loads and phytoplankton biomass. J. Great Lakes Res. 40, 496–501. http://dx.doi.org/10.1016/j.jglr.2014.04.004.

Kim, D.K., Zhang, W., Watson, S., Arhonditsis, G.B., 2014. A commentary on the modelling of the causal linkages among nutrient loading, harmful algal blooms, and hypoxia patterns in Lake Erie. J. Great Lakes Res. 40, 117–129. http://dx.doi.org/10.1016/j.jglr.2014.02.014.

Lam, D.C.L., Schertzer, W.M., Fraser, A.S., 1983. Simulation of Lake Erie Water Quality Responses to Loading and Weather Variations. Environment Canada, Scientific Series/Inland Waters Directorate; No. 134, Burlington, Ontario.

Lam, D., Schertzer, W., Fraser, A., 1987. A post-audit anaylsis of the NWRI nine-box water quality model for Lake Erie. J. Great Lakes Res. 13, 782–800.

Lam, D., Schertzer, W., McCrimmon, R., Charlton, M., Millard, S., 2008. Modeling Phosphorus and Dissolved Oxygen Conditions Pre- and Post-*Dreissena* Arrival in Lake Erie. In: Munawar, M., Heath, R. (Eds.), Checking the Pulse of Lake Erie. Aquatic Ecosystem Health and Management Society, Burlington, Ontario.

Leon, L.F., Smith, R.E.H., Hipsey, M.R., Bocaniov, S.A., Higgins, S.N., Hecky, R.E., Antenucci, J.P., Imberger, J.A., Guildford, S.J., 2011. Application of a 3D hydrodynamic-biological model for seasonal and spatial dynamics of water quality and phytoplankton in Lake Erie. J. Great Lakes Res. 37, 41–53.

Lesht, B.M., Fontaine, T.D., Dolan, D.M., 1991. Great Lakes Total Phosphorus Model: post audit and regionalized sensitivity analysis. J. Great Lakes Res. 17, 3–17. http://dx.doi.org/10.1016/S0380-1330(91)71337-3.

Liu, W., Bocaniov, S.A., Lamb, K.G., Smith, R.E.H., 2014. Three dimensional modeling of the effects of changes in meteorological forcing on the thermal structure of Lake Erie. J. Great Lakes Res. 40, 827–840.

Ludsin, S., Kershner, M., Blocksom, K., Knight, R., Stein, R., 2001. Life after death in Lake Erie: nutrient controls drive fish species richness, rehabilitation. Ecol. Appl. 11, 731–746.

Maccoux, M.J., Dove, A., Backus, S.M., Dolan, D.M., 2016. Total and soluble reactive phosphorus loadings to Lake Erie. J. Great Lakes Res. 42 (6), 1151–1165 (in this issue).
Michalak, A.M., Anderson, E.J., Beletsky, D., Boland, S., Bosch, N.S., Bridgeman, T.B., Chaffin, J.D., Cho, K., Confesor, R., Daloglu, I., Depinto, J., Evans, M.A., Fahnenstiel, G.L., He, L., Ho, J.C., Jenkins, L., Johengen, T.H., Kuo, K.C., Laporte, E., Liu, X., McWilliams, M.R., Moore, M.R., Posselt, D.J., Richards, R.P., Scavia, D., Steiner, A.L., Verhamme, E., Wright, D.M., Zagorski, M.A., 2013. Record-setting algal bloom in Lake Erie caused by agricultural and meteorological trends consistent with expected future conditions. Proc. Natl. Acad. Sci. U. S. A. 110, 6448–6452.
Obenour, D., Gronewold, A., Stow, C.A., Scavia, D., 2014. Using a Bayesian hierarchical model to improve Lake Erie cyanobacteria bloom forecasts. Water Resour. Res. 50, 7847–7860.
Oveisy, A., Rao, Y.R., Leon, L.F., Bocaniov, S.A., 2014. Three-dimensional winter modeling and the effects of ice cover on hydrodynamics, thermal structure and water quality in Lake Erie. J. Great Lakes Res. 40, 19–28.
Rinta-Kanto, J.M., Saxton, M.A., DeBruyn, J.M., Smith, J.L., Marvin, C.H., Krieger, K.A., Sayler, G.S., Boyer, G.L., Wilhelm, S.W., 2009. The diversity and distribution of toxigenic *Microcystis* spp. in present day and archived pelagic and sediment samples from Lake Erie. Harmful Algae 8, 385–394. http://dx.doi.org/10.1016/j.hal.2008.08.026.
Rucinski, D.K., Beletsky, D., DePinto, J.V., Schwab, D.J., Scavia, D., 2010. A simple 1-dimensional, climate based dissolved oxygen model for the central basin of Lake Erie. J. Great Lakes Res. 36, 465–476. http://dx.doi.org/10.1016/j.jglr.2010.06.002.
Rucinski, D.K., DePinto, J.V., Scavia, D., Beletsky, D., 2014. Modeling Lake Erie's hypoxia response to nutrient loads and physical variability. J. Great Lakes Res. 40, 151–161. http://dx.doi.org/10.1016/j.jglr.2014.02.003.
Rucinski, D., DePinto, J., Beletsky, D., Scavia, D., 2016. Modeling hypoxia in the Central Basin of Lake Erie under potential phosphorus load reduction scenarios. J. Great Lakes Res. 42 (6), 1206–1211 (in this issue).
Scavia, D., Justic, D., Bierman, V., 2004. Reducing hypoxia in the Gulf of Mexico: advice from three models. Estuaries 27, 419–425.
Scavia, D., Allan, J.D., Arend, K.K., Bartell, S., Beletsky, D., Bosch, N.S., Brandt, S.B., Briland, R.D., Daloğlu, I., DePinto, J.V., Dolan, D.M., Evans, M.A., Farmer, T.M., Goto, D., Han, H., Höök, T.O., Knight, R., Ludsin, S.A., Mason, D., Michalak, A.M., Richards, R.P., Roberts, J.J., Rucinski, D.K., Rutherford, E., Schwab, D.J., Sesterhenn, T.M., Zhang, H., Zhou, Y., 2014. Assessing and addressing the re-eutrophication of Lake Erie: central basin hypoxia. J. Great Lakes Res. 40, 226–246.
Scavia, D., DePinto, J.V., Auer, M., Bertani, I., Bocaniov, S., Chapra, S., Leon, L., McCrimmon, C., Obenour, D., Peterson, G., Rucinski, D., Schlea, D., Steger, C., Stumpf, R., Yerubandi, R., Zhang, H., 2016. Great Lakes Water Quality Agreement Nutrient Annex Objectives and Targets Task Team Ensemble Multi-Modeling Report. Great Lakes National Program Office, USEPA, Chicago (https://www.epa.gov/sites/production/files/2016-09/documents/nutrientannex4multimodelingreportfinal31aug2016.pdf).
Stow, C., Roessler, C., Borsuk, M., Bowen, J., Reckhow, K., 2003. Comparison of estuarine water quality models for total maximum daily load development in Neuse River estuary. J. Water Resour. Plan. Manag. 129, 307–314.
Stow, C.A., Cha, Y., Johnson, L.T., Confesor, R., Richards, R.P., 2015. Long-term and seasonal trend decomposition of Maumee River nutrient inputs to western Lake Erie. Environ. Sci. Technol. 49, 3392–3400. http://dx.doi.org/10.1021/es5062648.
Stumpf, R.P., Wynne, T.T., Baker, D.B., Fahnenstiel, G.L., 2012. Interannual variability of cyanobacterial blooms in Lake Erie. PLoS One 7, e42444.
Stumpf, R.P., Johnson, L.T., Wynne, T.T., Baker, D.B., 2016. Forecasting annual cyanobacterial bloom biomass to inform management decisions in Lake Erie. J. Great Lakes Res. 42 (6), 1174–1183 (in this issue).
Task Team, 2015. Recommended Phosphorus Loading Targets for Lake Erie. Annex 4 Objectives and Targets Task Team Final Report to the Nutrients Annex Subcommittee (May 2015. http://tinyurl.com/pcvwt8g).
Tomlinson, L., Auer, M., Bootsma, H., 2010. The Great Lakes Cladophora model: development and application to Lake Michigan. J. Great Lakes Res. 36, 287–297.
Valipour, R., Leon, L., Depew, D., Dove, A., Rao, Y., 2016. High-resolution modeling for development of nearshore ecosystem objectives in eastern Lake Erie. J. Great Lakes Res. 42 (6), 1241–1251 (in this issue).
Vallentyne, J.R., Thomas, N.A., 1978. Fifth Year Review of Canada–United State Great Lakes Water Quality Agreement. Report of Task Group III. A Technical Group to Review Phosphorus Loadings.
Vanderploeg, H.A., Liebig, J.R., Carmichael, W.W., Agy, M.A., Johengen, T.H., Fahnenstiel, G.L., Nalepa, T.F., 2001. Zebra mussel (*Dreissena polymorpha*) selective filtration promoted toxic Microcystis blooms in Saginaw Bay (Lake Huron) and Lake Erie. Can. J. Fish. Aquat. Sci. 58, 1208–1221.
Verhamme, E., Redder, T., Schlea, D., Grush, J., Bratton, J., DePinto, J., 2016. Development of the Western Lake Erie Ecosystem Model (WLEEM): application to connect phosphorus loads to cyanobacteria biomass. J. Great Lakes Res. 42 (6), 1193–1205 (in this issue).
Vollenweider, R., 1976. Advances in defining critical loading levels for phosphorus in lake eutrophication. Mem. dell'Istituto Ital. di Idrobiol. 33, 53–83.
Weller, D.E., Benham, B., Friedrichs, M., Najjar, R., Paolisso, M., Pascual, P., Shenk, G., Sellner, K., 2013. Multiple Models for Management in the Chesapeake Bay. STAC Publication Number 14-004, Edgewater, MD, p. 37.
Young, T.C., Depinto, J.V., Martin, S.C., Bonner, J.S., 1985. Algal-available particulate phosphorus in the Great Lakes Basin. J. Great Lakes Res. 11, 434–446.
Zhang, H., Culver, D.a., Boegman, L., 2008. A two-dimensional ecological model of Lake Erie: application to estimate dreissenid impacts on large lake plankton populations. Ecol. Model. 214, 219–241. http://dx.doi.org/10.1016/j.ecolmodel.2008.02.005.
Zhang, H., Culver, D., Boegman, L., 2011. Dreissenids in Lake Erie: an algal filter or a fertilizer? Aquat. Invasions 6, 175–194.
Zhang, H., Culver, D., Boegman, L., 2016. Spatial distributions of external and internal phosphorus loads and their impacts on Lake Erie's phytoplankton. J. Great Lakes Res. 42 (6), 1212–1227 (in this issue).
Zhou, Y., Obenour, D.R., Scavia, D., Johengen, T.H., Michalak, A.M., 2013. Spatial and temporal trends in Lake Erie hypoxia, 1987–2007. Environ. Sci. Technol. 47, 899–905. http://dx.doi.org/10.1021/es303401b.